Inorg. Chem. **2002**, *41*, 4149–4157

Synthesis and Characterization of Iron Complexes with Monoanionic and Dianionic *N,N′,N″*-Trialkylguanidinate Ligands

Stephen R. Foley, Glenn P. A. Yap, and Darrin S. Richeson*

Department of Chemistry, University of Ottawa, Ottawa, ON K1N 6N5, Canada

Received January 29, 2002

Trisubstitued *N,N′,N″*-tri(alkyl)guanidinate anions have been used in the synthesis of a family of Fe(II) and Fe(III) complexes. Complexes $FeCl\{(^iPrN)_2C(HN^iPr)\}_2$ (**1**), $[Fe\{\mu\text{-}(^iPrN)_2C(HN^iPr)\}\{(^iPrN)_2C(HN^iPr)\}]_2$ (**2**), and $[Fe\{\mu\text{-}(CyN)_2C(HNCy)\}\{(CyN)_2C(HNCy)\}]_2$ (**3**) were prepared from the reaction of the appropriate lithium tri(alkyl)guanidinate and $FeCl_3$ or $FeBr_2$. The complex $[FeBr\{\mu\text{-}(CyN)_2C(HNCy)\}]_2$ (**4**), an apparent intermediate in the formation of **3**, has also been isolated and characterized. Complexes **1** and **2** react with alkyllithium reagents to yield products that depend on the identity of the reagent as well as the reaction stoichiometry. Reaction of **2** with MeLi (1:2 ratio) produces $Li_2[Fe\{\mu\text{-}(^iPrN)_2C{=}N^iPr\}\{(^iPrN)_2C(HN^iPr)\}]_2$ (**5**). Reaction of **1** with an equimolar amount of $LiCH_2SiMe_3$ results in reduction to Fe(II) and generation of **2** while reaction with 4 $LiCH_2SiMe_3$ proceeds by a combination of reduction, substitution, and deprotonation of guandinate to yield $Li_4(THF)_2[Fe\{(^iPrN)_2CN^iPr\}(CH_2SiMe_3)_2]_2$ (**7**). Both complexes **5** and **7** posssess dianionic guanidinate ligands. The reaction of **2** with 1 equiv of $LiCH_2SiMe_3$ generated $Fe_2\{\mu\text{-}(^iPrNCN^iPr)_2(N^iPr)\}\{(^iPrN)_2C(HN^iPr)\}_2$ (**6**). Compound **6** has a dianionic biguanidinate ligand derived from the coupling of the two bridging guanidinate ligands of **2**.

Introduction

Guanidinate mono- and dianions are sterically and electronically flexible ancillary ligands that are receiving increasing attention in organometallic and coordination chemistry. Recently, the transition metal chemistry of guanidinates has flourished and the versatility of these species as ligands is beginning to be demonstrated for a wide range of metals.[1−7] We are interested in revealing the coordination properties of *N,N′,N″*-trialkylguanidinate anions (Chart 1) and in exploiting the potential of dianionic species generated by deprotonation of the second N−H function.

Chart 1

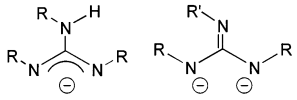

The relative scarcity of Fe complexes supported with anionic nitrogen-centered ligands warrants an exploration of the ability of guanidinate ligands to function in this regard. Interestingly, the first transition metal complexes of dianionic guanidinate ligands are the dinuclear iron species $[\mu^2\text{-}(RN)_3C][Fe(CO)_3]_2$ (**A**: R = Cy, ^{i}Pr).[8] These remained as unique examples of transition meal coordinated guanidinate dianions

* E-mail: darrin@science.uottawa.ca.

(1) Bailey, P. J.; Pace, S. *Coord. Chem. Rev.* **2001**, *214*, 91 and references therein.
(2) Duncan, A. P.; Mullins, S. M.; Arnold, J.; Bergman, R. G. *Organometallics* **2001**, *20*, 1808. Mullins, S. M.; Duncan, A. P.; Bergman, R. G.; Arnold, J. *Inorg. Chem.* **2001**, *40*, 6952.
(3) Lu, Z.; Yap, G. P. A.; Richeson, D. S. *Organometallics* **2001**, *20*, 706.
(4) Thirupathi, N.; Yap, G. P. A.; Richeson, D. S. *Organometallics* **2000**, *19*, 2573. Thirupathi, N.; Yap, G. P. A.; Richeson, D. S. *J. Chem. Soc., Chem. Commun.* **1999**, 2483.
(5) Ong, T.-G.; Wood, D.; Yap, G. P. A.; Richeson, D. S. *Organometallics* **2002**, *21*, 1.
(6) Foley, S. R.; Yap, G. P. A.; Richeson, D. S. *J. Chem. Soc., Chem. Commun.* **2000**, 1515.
(7) For recently published complexes with the guanidinate anion derived from 1,3,4,6,7,8-hexahydro-2*H*-pyrimido[1,2-*a*]pyrimidine (hpp^-) see: Coles, M. P.; Hitchcock, P. B. *J. Chem. Soc., Dalton Trans.* **2001**, 1169 and references therein. Clerac, R.; Cotton, F. A.; Daniels, L. M.; Donahue, J. P.; Murillo, C. A.; Timmons, D. J. *Inorg. Chem.* **2000**, *39*, 2581−2584 and references therein. Cotton, F. A.; Murillo, C. A.; Wang, X. P. *Inorg. Chim. Acta* **2000**, *300*, 1−6 and references therein. Cotton, F. A.; Gu, J. D.; Murillo, C. A.; Timmons, D. J. *J. Chem. Soc., Dalton Trans.* **1999**, 3741−3745 and references therein. Cotton, F. A.; Murillo, C. A.; Timmons, D. J. *Chem. Commun.* **1999**, 1427−1428 and references therein. Cotton, F. A.; Matonic, J. H.; Murillo, C. A. *J. Am. Chem. Soc.* **1998**, *120*, 6047−6052 and references therein.
(8) Bremer, N. J.; Cutcliffe, A. B.; Farona, M. F. *Chem. Commun.* **1970**, 932.

10.1021/ic020088c CCC: $22.00
Published on Web 07/12/2002

Scheme 1

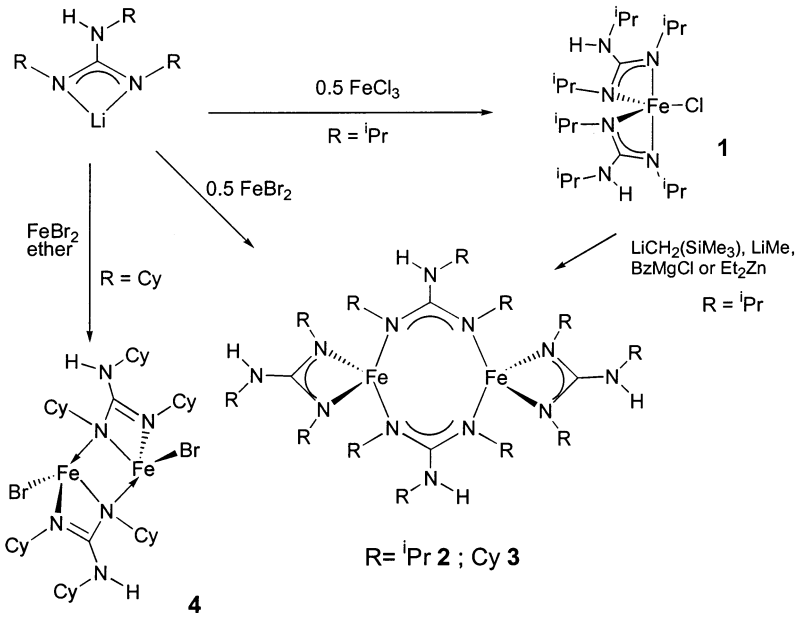

until 1996 when Pt[$(NPh)_2C$═NPh](COD) (COD = cyclooctadiene) was isolated and characterized.[9]

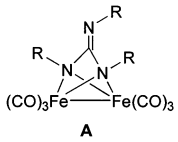

The application of related amidinate ligands in the preparation of Fe complexes has experienced varying degrees of success.[10−12] From these reports it seems clear that this chemistry is complex and that the products obtained show a dependence on choice of ligand, choice of starting material, and even the identity of the alkyllithium reagent employed in the ligand deprotonation.

We now present our results for the application of *N*,*N*′,*N*″-trisubstituted guanidinates as ligands for Fe(II) and Fe(III) complexes including more complete details of our initially communicated results.[6] Included are the essential experimental features for the synthesis and characterization of FeCl{(^{i}PrN)$_2$C(HN^{i}Pr)}$_2$ (**1**) and [Fe{μ-(^{i}PrN)$_2$C(HN^{i}Pr)}{(^{i}PrN)$_2$C(HN^{i}Pr)}]$_2$ (**2**), and the extension of this chemistry to the cyclohexyl (Cy) analogue of **2**, [Fe{μ-(CyN)$_2$C(HNCy)}{(CyN)$_2$C(HNCy)}]$_2$ (**3**). An apparent intermediate in the formation of **3**, [FeBr{μ-(CyN)$_2$C(HNCy)}]$_2$ (**4**), has been isolated and characterized. The products of the reactions of **1** and **2** with alkyllithium reagents depend on the identity of the reagent as well as the reaction stoichiometry and include the dianionic guanidinate complexes Li$_2$[Fe{μ-(^{i}PrN)$_2$C═N^{i}Pr}{(^{i}PrN)$_2$C(HN^{i}Pr)}]$_2$ (**5**) and Li$_4$(THF)$_2$[Fe{(^{i}PrN)$_2$CN^{i}Pr}(CH$_2$SiMe$_3$)$_2$]$_2$ (**7**) as well as the product derived from the coupling of the two bridging guanidinate ligands Fe$_2${μ-(^{i}PrNCN^{i}Pr)$_2$(N^{i}Pr)}{(^{i}PrN)$_2$C(HN^{i}Pr)}$_2$ (**6**).

Results and Discussion

Fe(II/III) Complexes of *N*,*N*′,*N*″-Tri(alkyl)guanidinate Monoanions. The lithium *N*,*N*′,*N*″-tri(alkyl)guanidinate Li{(RN)$_2$C(HNR)} (R = ^{i}Pr, Cy) starting materials were formed by direct reaction of the appropriate guanidine with 1 equiv of either MeLi or ^{n}BuLi. In all cases, freshly prepared solutions of lithium guanidinate were employed in the metathesis reactions with iron halides (Scheme 1).

The addition of 0.5 equiv of FeCl$_3$ to a solution of Li{(^{i}PrN)$_2$C(HN^{i}Pr)} followed by recrystallization from pentane resulted in isolation of the bis(guanidinate) iron(III) chloride complex FeCl{(^{i}PrN)$_2$C(HN^{i}Pr)}$_2$, **1**.[13] The distorted pseudo-trigonal-bipyramidal geometry exhibited by **1** was approximately of C_2 symmetry. The average Fe−N$_{axial}$ bond distances of 2.085(3) Å are slightly longer than the average Fe−N$_{equat}$ distances of 2.008(3) Å. Within the chelating NCN moieties, the C−N bond distances (average = 1.34, 1.36 Å) are consistent with partial double bond character.

Attempts to exchange the chloro ligand of **1** with an alkyl group by using MeLi, LiCH$_2$(SiMe$_3$), ZnEt$_2$, or BzMgCl led, in all cases, to reduction of the metal center from Fe(III) to Fe(II) and formation of complex **2** in 40−80% yields (Scheme 1). Single-crystal X-ray analysis of **2** provided a formula of [Fe{μ-(^{i}PrN)$_2$C(HN^{i}Pr)}{(^{i}PrN)$_2$C(HN^{i}Pr)}]$_2$ and showed it to be a dinuclear species with two bridging guanidinate ligands and two chelating bidentate ligands.[13,14] A direct, higher yield (82%) route to **2** is provided by the reaction of FeBr$_2$ with 2 equiv of Li{(^{i}PrN)$_2$C(HN^{i}Pr)}.

(9) Dinger, M. B.; Henderson, W. *Chem. Commun.* **1996**, 212.
(10) Clark, J. A.; Kilner, M.; Pietrzykowski, A. *Inorg. Chim. Acta* **1984**, *82*, 85.
(11) Zinn, A.; von Arnim, H.; Massa, W.; Shafer, M.; Pebler, J.; Dehnicke, K. *Z. Naturforsch.* **1991**, *46B*, 1300.
(12) (a) Cotton, F. A.; Daniels, L. M.; Matonic, J. C.; Murillo, C. A. *Inorg. Chim. Acta*, **1997**, *256*, 277. (b) Cotton, F. A.; Daniels, L. M.; Maloney, D. J.; Murillo, C. A. *Inorg. Chim. Acta* **1996**, *252*, 293. (c) Cotton, F. A.; Daniels, L. M.; Murillo, C. A. *Inorg. Chim. Acta* **1994**, *224*, 5. (d) Cotton, F. A.; Daniels, L. M.; Falvello, L. R.; Murillo, C. A. *Inorg. Chim. Acta* **1994**, *219*, 7.

(13) The structural details of complexes **1**, **2**, and **6** were previously reported in ref 6.

Table 1. Crystal Data for Compounds **3**−**5** and **7**

	3	**4**	**5**	**7**
formula	$C_{76}H_{136}Fe_2N_{12}(THF)_{1.5}$	$C_{38}H_{68}Br_2Fe_2N_6$	$C_{40}H_{86}Fe_2Li_2N_{12}$	$C_{44}H_{102}Fe_2Li_4N_6O_2Si_4$
fw	1437.82	880.50	860.79	999.14
temp (K)	203(2)	203(2)	238(2)	238(2)
λ (Å)	0.71073	0.71073	0.71073	0.71073
space group	$P\bar{1}$	$P2_1/c$	$P\bar{1}$	$P2_1/n$
a (Å)	14.283(1)	11.732(1)	9.944(3)	16.410(9)
b (Å)	14.437(1)	15.402(1)	9.946(3)	11.398(6)
c (Å)	23.517(2)	12.893(1)	13.775(4)	17.380(10)
α (deg)	86.821(2)		73.201(5)	
β (deg)	72.475(2)	113.110(1)	82.316(5)	107.013(7)
γ (deg)	63.664(1)		73.183(5)	
V (Å^3)	4127.1(7))	2142.7(3)	1246.5(7)	3108(3)
Z	2	2	1	2
d_{calcd} (g/cm^3)	1.157	1.365	1.147	1.068
abs coeff (mm^{-1})	0.402	2.574	0.620	0.578
R1[a]	0.0508	0.0386	0.0480	0.0422
wR2[b]	0.1231	0.0750	0.1107	0.0944

[a] $R1 = \sum||F_o| - |F_c||/\sum|F_o|$. [b] $wR2 = (\sum w(|F_o| - |F_c|)^2/\sum w|F_o|^2)^{1/2}$.

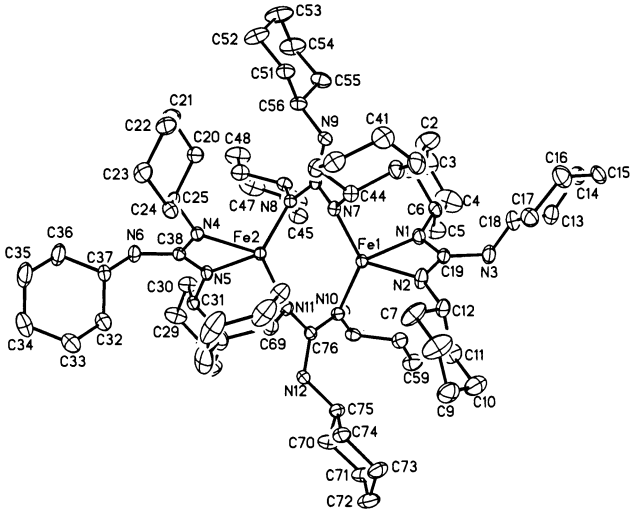

Figure 1. Molecular structure of [Fe{μ-(CyN)$_2$C(HNCy)}{(CyN)$_2$C(HNCy)}]$_2$ (**3**) with the atom numbering scheme. Hydrogen atoms have been omitted for clarity.

A similar reaction of $FeBr_2$ with 2 equiv of Li{(CyN)$_2$C(HNCy)} led to the successful isolation of [Fe{μ-(CyN)$_2$C(HNCy)}{(CyN)$_2$C(HNCy)}]$_2$ (**3**, Scheme 1). The formulation of complex **3** was confirmed through a single-crystal X-ray diffraction study (Table 1). Figure 1 and Table 2 provide a summary of these results. The structure of this dinuclear Fe(II) complex is akin to that of **2** with four monoanionic guanidinate ligands in two different coordination modes. Two of the ligands bridge the Fe(II) centers while the other two guanidinates chelate to different iron atoms. The coordination spheres for the two Fe centers in **3** are composed of four nitrogen centers of the two different ligands. The N−Fe−N bond angles vary from 63.1° for the chelating ligands to 134.1° for the bridging ligands with an average value of 106°. The Fe−N bond distances span a range from 2.033(2) to 2.134(2) Å.

Table 2. Selected Bond Distances [Å] and Angles [deg] for **3**

	Distances		
Fe(1)−N(10)	2.050(2)	N(5)−C(38)	1.328(4)
Fe(1)−N(7)	2.050(2)	N(5)−C(31)	1.459(4)
Fe(1)−N(2)	2.112(3)	N(6)−C(38)	1.416(4)
Fe(1)−N(1)	2.122(2)	N(6)−C(37)	1.465(4)
Fe(2)−N(8)	2.033(2)	N(7)−C(57)	1.352(4)
Fe(2)−N(11)	2.056(2)	N(7)−C(44)	1.473(4)
Fe(2)−N(4)	2.123(2)	N(8)−C(57)	1.325(4)
Fe(2)−N(5)	2.134(2)	N(8)−C(50)	1.472(4)
N(1)−C(19)	1.322(4)	N(9)−C(57)	1.382(4)
N(1)−C(6)	1.459(4)	N(9)−C(56)	1.462(4)
N(2)−C(19)	1.327(4)	N(10)−C(76)	1.323(3)
N(2)−C(12)	1.458(4)	N(10)−C(63)	1.478(4)
N(3)−C(19)	1.402(4)	N(11)−C(76)	1.343(4)
N(3)−C(18)	1.414(5)	N(11)−C(69)	1.470(4)
N(4)−C(38)	1.321(4)	N(12)−C(76)	1.393(3)
N(4)−C(25)	1.469(4)	N(12)−C(75)	1.475(4)
	Angles		
N(10)−Fe(1)−N(7)	134.05(9)	N(1)−C(19)−N(3)	123.1(3)
N(10)−Fe(1)−N(2)	108.20(11)	N(2)−C(19)−N(3)	123.4(3)
N(7)−Fe(1)−N(2)	109.40(11)	C(38)−N(6)−C(37)	118.0(2)
N(10)−Fe(1)−N(1)	115.93(10)	C(57)−N(7)−C(44)	124.2(2)
N(7)−Fe(1)−N(1)	104.18(10)	C(57)−N(7)−Fe(1)	111.52(19)
N(2)−Fe(1)−N(1)	63.09(10)	C(44)−N(7)−Fe(1)	119.42(18)
N(8)−Fe(2)−N(11)	129.10(9)	C(57)−N(8)−C(50)	122.0(2)
N(8)−Fe(2)−N(4)	107.52(9)	C(57)−N(8)−Fe(2)	111.38(19)
N(11)−Fe(2)−N(4)	117.01(9)	C(50)−N(8)−Fe(2)	126.58(19)
N(8)−Fe(2)−N(5)	114.35(9)	C(57)−N(9)−C(56)	128.8(3)
N(11)−Fe(2)−N(5)	107.18(9)	C(76)−N(10)−C(63)	120.7(2)
N(4)−Fe(2)−N(5)	63.07(9)	C(76)−N(10)−Fe(1)	107.72(19)
C(19)−N(1)−C(6)	123.4(3)	C(63)−N(10)−Fe(1)	129.80(18)
C(19)−N(1)−Fe(1)	91.56(18)	C(76)−N(11)−C(69)	118.8(2)
C(6)−N(1)−Fe(1)	145.0(2)	C(76)−N(11)−Fe(2)	118.36(18)
C(19)−N(2)−C(12)	122.2(3)	C(69)−N(11)−Fe(2)	121.07(18)
C(19)−N(2)−Fe(1)	91.86(19)	C(76)−N(12)−C(75)	126.0(2)
C(12)−N(2)−Fe(1)	145.0(2)	N(4)−C(38)−N(5)	114.4(3)
C(19)−N(3)−C(18)	120.8(3)	N(4)−C(38)−N(6)	122.9(3)
C(38)−N(4)−C(25)	121.8(2)	N(5)−C(38)−N(6)	122.7(3)
C(38)−N(4)−Fe(2)	91.64(18)	N(8)−C(57)−N(7)	116.0(3)
C(25)−N(4)−Fe(2)	142.89(18)	N(8)−C(57)−N(9)	124.4(3)
C(38)−N(5)−C(31)	121.9(2)	N(7)−C(57)−N(9)	119.6(3)
C(38)−N(5)−Fe(2)	90.93(17)	N(10)−C(76)−N(11)	117.5(3)
C(31)−N(5)−Fe(2)	143.85(19)	N(10)−C(76)−N(12)	123.1(3)
N(1)−C(19)−N(2)	113.5(3)	N(11)−C(76)−N(12)	119.3(2)

The two chelating bidentate guanidinates are planar and exhibit bonding parameters reminiscent of other complexes with chelating monoanionic guanidinates such as **1** and **2**.[6] The bridging guanidinate ligands are also planar; they exhibit planar central C atoms (C(57), C(76)) and the four N centers

(14) For recently reported examples of structurally characterized carboxylate-bridged diiron(II) complexes see: Lee, D.; Lippard, S. J. *Inorg. Chem.* **2002**, *41*, 827 and references therein. Lecloux, D. D.; Barrios, A. M.; Mizoguchi, T. J.; Lippard, S. J. *J. Am. Chem. Soc.* **1998**, *120*, 9001 and references therein.

Chart 2

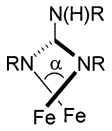

coordinated to Fe (N(7), N(8), N(10), N(11)) deviate only very slightly from planarity. The CN bond distances within the bridging groups are indicative of delocalized π-bonding (N(7)−C(57) 1.352(4) Å, N(8)−C(57) 1.325(4) Å, N(10)−C(76) 1.323(3) Å, N(11)−C(76) 1.343(4) Å). The C−N(H)-Cy bond lengths for the bridging ligands have an average value of 1.47 Å as expected for a CN single bond.

While the bridging ligands are planar, their coordination to the diiron core generates a twisted configuration as measured by the dihedral angle, α, represented in Chart 2. These angles in **3**, defined by Fe(1)−N(10)−N(11)−Fe(2) and Fe(1)−N(7)−N(8)−Fe(2), have values of 70.0° and 73.6° respectively.

Complexes **2** and **3** have some analogous structural features with the amidinate complex $Fe_2(\mu\text{-DPhBz})_2(DPhBz)_2$ (**B**: DPhBz = *N*,*N*′-diphenylbenzamidinate) including a similar distortion of the bridging ligand.[12a,15] The observed geometry of **B** was attributed to a weak intramolecular

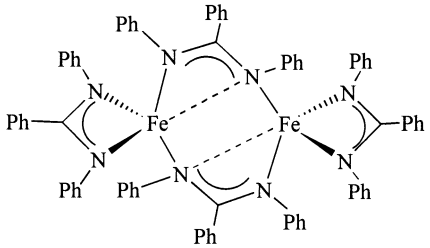

B

Fe···N interaction at a distance of 2.477(4) Å. For **2**, the closest nonbonded N to Fe distances are the transannular distances Fe(1)−N(11) and Fe(2)−N(7) at 2.970 and 3.007 Å, respectively.[6] For **3** these distances are even greater with the two shortest contacts being Fe(1)−N(8) at 3.050 Å and Fe(2)−N(10) at 3.190 Å. In both **2** and **3** these distances are considerably greater than those observed for **B** and are not likely the result of a significant interaction between these atoms. The possibility of an Fe−Fe bond in either **2** or **3** is excluded by the large iron−iron separation of 3.264 and 3.161 Å, respectively. [12a,c,16] The magnetic moments for **2** and **3** of 7.50μ_B and 7.28 μ_B are consistent with two antiferromagnetically coupled high-spin Fe(II) centers.

A related dinuclear molybdenum complex $Mo_2[\mu\text{-}(NPh)_2\text{-}CNHPh]_4$ has been prepared with a tri(phenyl)guanidinate ligand.[17] This species displayed a Mo−Mo bond and four

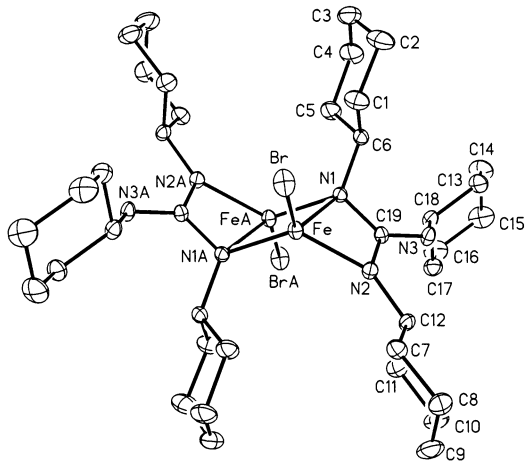

Figure 2. Molecular structure of $[FeBr\{\mu\text{-}(CyN)_2C(HNCy)\}]_2$ (**4**) with the atom numbering scheme. Hydrogen atoms have been omitted for clarity.

Table 3. Selected Bond Distances [Å] and Angles [deg] for **4**

	Distances		
Br−Fe	2.3891(4)	N(1)−C(6)	1.495(3)
Fe−N(1)A	2.0347(18)	N(2)−C(19)	1.315(3)
Fe−N(2)	2.0363(18)	N(2)−C(12)	1.473(3)
Fe−N(1)	2.2557(17)	N(3)−C(19)	1.355(3)
Fe−FeA	2.8399(6)	N(3)−C(18)	1.465(3)
N(1)−C(19)	1.390(3)		
	Angles		
N(1)A−Fe−N(2)	116.91(7)	C(6)−N(1)−FeA	119.28(13)
N(1)A−Fe−N(1)	97.28(6)	C(19)−N(1)−Fe	85.57(12)
N(2)−Fe−N(1)	63.44(7)	C(6)−N(1)−Fe	126.63(13)
N(1)A−Fe−Br	116.55(5)	FeA−N(1)−Fe	82.72(6)
N(2)−Fe−Br	122.37(5)	C(19)−N(2)−C(12)	121.39(18)
N(1)−Fe−Br	127.45(5)	C(19)−N(2)−Fe	97.08(13)
N(1)A−Fe−FeA	51.99(5)	C(12)−N(2)−Fe	141.51(14)
N(2)−Fe−FeA	88.23(5)	C(19)−N(3)−C(18)	125.31(19)
N(1)−Fe−FeA	45.29(5)	N(2)−C(19)−N(3)	124.6(2)
Br−Fe−FeA	143.44(2)	N(2)−C(19)−N(1)	113.61(18)
C(19)−N(1)−C(6)	115.68(17)	N(3)−C(19)−N(1)	121.76(19)
C(19)−N(1)−FeA	118.76(14)		

planar bridging guanidinate ligands. Unlike **2** and **3**, the Mo−Mo vector is coplanar with the bridging ligand (α = 0).

We were interested in the possibility of isolating intermediate species in the synthesis of **2** and **3** and therefore attempted the stepwise introduction of guanidinate ligand to $FeBr_2$. When lithium *N*,*N*′,*N*″-tricyclohexylguanidinate, Li-$\{(CyN)_2C(HNCy)\}$, was reacted with $FeBr_2$ in a 1:1 ratio complex **4** was isolated (Scheme 1). X-ray crystallography (Table 1) confirmed the identity of this compound as $[FeBr\{\mu\text{-}(CyN)_2C(HNCy)\}]_2$ as shown in Figure 2. Bond distances and angles for **4** are summarized in Table 3. Complex **4** is a dinuclear Fe(II) complex where the two metal centers are held in proximity by two bridging monoanionic guanidinate ligands. A terminal bromide completes the pseudotetrahedral coordination environment of each iron center.

Examination of the structural features of **4** reveals that in contrast to **2** and **3** with bridging bidentate ligand coordina-

(15) A similar distortion has also been reported in a rhodium triazenide complex: Connelly, N. G.; Hopkins, P. M.; Orpen, A. G.; Rosair, G. M.; Viguri, F. *J. Chem. Soc., Dalton. Trans.* **1992**, 2907.

(16) For examples of complexes with Fe−Fe bonds see: (a) $Fe_2(CO)_9$ with single bond Fe−Fe = 2.523 Å. (b) Walther, B.; Harting, H.; Reinhold: J.; Jones, P. G.; Mealli, C.; Böttcher, H.-C.; Baumeister, U.; Krug, A.; Möckel, A. *Organometallics* **1992**, *11*, 1542. (c) Cotton, F. A.; Daniels, L. M.; Falvello, L. R.; Matonic, J. H.; Murillo, C. A. *Inorg. Chim. Acta* **1997**, *256*, 269. (d) Klose, A.; Solari, E.; Floriani, C.; Chiesi-Villa, A.; Rizzoli, C.; Re, N. *J. Am. Chem. Soc.*, **1994**, *I16*, 9123. (e) Klose, A.; Solari, E.; Ferguson, R.; Floriani, C.; Chiesi-Villa, A.; Rizzoli, C. *Organometallics* **1993**, *12*, 2414.

(17) Bailey, P. J.; Bone, S. F.; Mitchell, L. A.; Parsons, S.; Taylor, K. J.; Yellowlees, L. J. *Inorg. Chem.* **1997**, *36*, 867. Bailey, P. J.; Bone, S. F.; Mitchell, L. A.; Parsons, S.; Taylor, K. J.; Yellowlees, L. J. *Inorg. Chem.* **1997**, *36*, 5420.

Chart 3

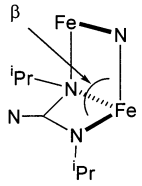

tion modes, this species is best described as having a chelating bidentate monoanionic guanidinate ligand with an additional longer range Fe−N interaction between two [FeBr{μ-(CyN)$_2$C(HNCy)}] units. In other words, Fe−N(1) and Fe−N(2) are the shortest Fe−N distances in the molecule and are similar in length at 2.035(2) and 2.036(2) Å, respectively. The Fe−N(1A) distance is considerably longer at 2.256(2) Å, but certainly well within the sum of the van der Waals radii of these atoms. This longer distance interaction generates the observed dinuclear structure. It also brings the two Fe atoms in closer proximity to each other than in **2** and **3**. However, the Fe−Fe distance of 2.8399(6) Å is still too long to be considered a significant metal−metal interaction.[12a,c,16] The magnetic moment of 8.63μ_B obtained for **4** suggests two independent high-spin Fe(II) centers in this compound. As a result of this atomic arrangement the molecular frame exhibits a planar four-membered ring for the Fe−N(1)−Fe(1)−N(1A) atoms. At an angle of 62.6° (β in Chart 3) with this plane is the plane formed by the chelating ligand Fe−N(1)−C(19)−N(2) ($\sum$ of internal angles = 359.7°).

Fe(II) Complexes of *N,N′,N″*-Tri(alkyl)guanidinate Dianions. Trisubstituted guanidinate monoanions have an additional N−H moiety that might be deprotonated. With this in mind we attempted to generate Fe(II) complexes with dianionic guanidinate ligands by reaction of **2** with strong bases. Complex **2** reacts rapidly with 2 equiv of MeLi in THF which, followed by recrystallization from pentane, results in the formation of Li$_2$[Fe{μ-(^{i}PrN)$_2$C=N^{i}Pr}{(^{i}PrN)$_2$C(HN^{i}Pr)}]$_2$ (**5**, Scheme 2).

Again, X-ray crystallography provided the structural identity for **5** (Table 1). Examination of Figure 3 in conjunction with the structural parameters summarized in Table 4 reveals that this new dinuclear Fe(II) complex is derived from the double deprotonation of complex **2**. Complex **5** exhibits two dianionic guanidinate ligands that bridge the two Fe centers while the two remaining monoanionic ligands now coordinate to Fe in a monodentate fashion. Since this reaction is not accompanied by any change

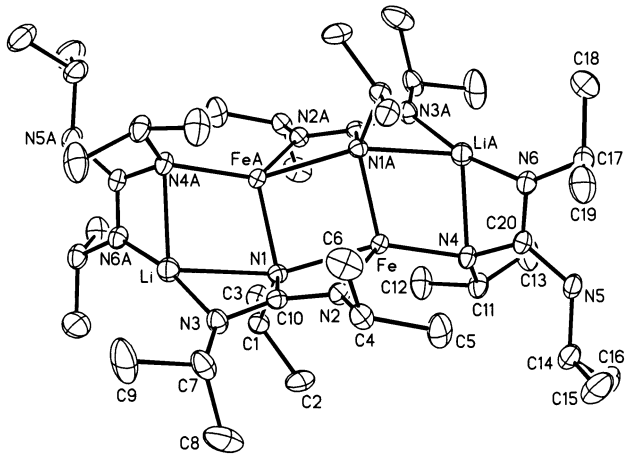

Figure 3. Molecular structure of Li$_2$[Fe{μ-(^{i}PrN)$_2$C=N^{i}Pr}{(^{i}PrN)$_2$C-(HN^{i}Pr)}] (**5**) with the atom numbering scheme. Hydrogen atoms have been omitted for clarity.

in Fe oxidation state, two lithium cations are required for charge balance. These Li cations are coordinated to the monoanionic guanidinate in a bidentate fashion and to two of the N centers of one of the dianionic guanidinates as indicated.

The structural core of **5** exhibits similarities with that of compound **4** with the replacement of the monoanionic bridging ligand for a dianionic analogue. Complex **5** possesses a crystallographic inversion center that generates the full molecule from the asymmetric unit, Li[Fe{μ-(^{i}PrN)$_2$C=N^{i}Pr}{(^{i}PrN)$_2$C(HN^{i}Pr)}]. Other similarities between **4** and **5** include the disposition of the bridging ligands with respect to the Fe$_2$ core, the short bonding interactions of Fe−N(1) and Fe−N(2) (2.093(2) and 2.030(2) Å), and an additional bonding interaction of each Fe center with a third nitrogen (Fe−N(1A) 2.235(2) Å). Again, this arrangement generates a four-membered planar (FeN)$_2$ rectangle and the additional nitrogen interaction preserves a distorted pseudotetrahedral environment about each iron center.

The dianionic guanidinate ligands in **5** are planar and parallel to each other. The β angle (Chart 3) between the Fe−N(1)−C(10)−N(2) mean plane and the Fe−Fe(A)−N1 mean plane is 59.6°.

The observed interactions of the guanidinate dianion with the two Fe centers should, as was seen with **4**, also lead to a localized π-bond within the chelating N−C−N group. This appears to be the case with the C−N distance for the tetracoordinated nitrogen center being consistent with a single bond (C(10)−N(1) 1.457(3) Å) while the CN bond distance

Scheme 2

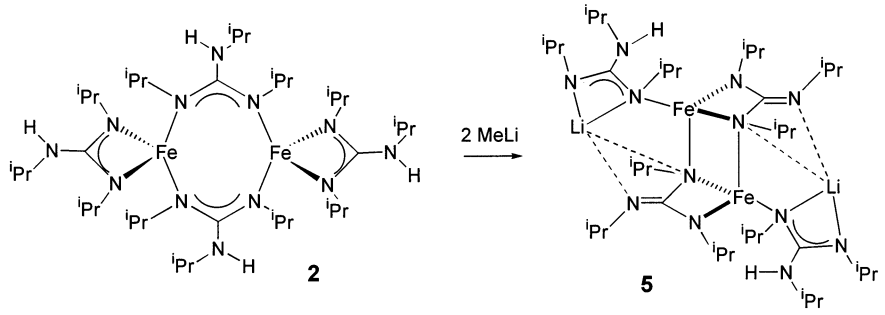

Table 4. Selected Bond Distances [Å] and Angles [deg] for **5**

		Distances	
Fe−N(2)	2.0304(18)	N(3)−C(7)	1.464(3)
Fe−N(4)	2.0524(18)	N(3)−Li	1.952(5)
Fe−N(1)A	2.0931(18)	N(4)−C(20)	1.385(3)
Fe−N(1)	2.2351(18)	N(4)−C(11)	1.484(3)
Fe−LiA	2.764(4)	N(5)−C(20)	1.376(3)
N(1)−C(10)	1.457(3)	N(5)−C(14)	1.455(3)
N(1)−C(1)	1.494(3)	N(6)−C(20)	1.309(3)
N(1)−Li	2.298(4)	N(6)−C(17)	1.469(3)
N(2)−C(10)	1.341(3)	Li−N(6)A	1.976(5)
N(2)−C(4)	1.467(3)	Li−N(4)A	2.214(4)
N(3)−C(10)	1.315(3)		
		Angles	
N(2)−Fe−N(4)	126.71(7)	C(11)−N(4)−LiA	113.26(19)
N(2)−Fe−N(1)A	119.39(7)	Fe−N(4)−LiA	80.66(11)
N(4)−Fe−N(1)A	106.01(7)	C(20)−N(5)−C(14)	128.5(2)
N(2)−Fe−N(1)	64.21(7)	C(20)−N(6)−C(17)	121.36(19)
N(4)−Fe−N(1)	142.31(7)	C(20)−N(6)−LiA	92.74(19)
N(1)A−Fe−N(1)	92.91(6)	C(17)−N(6)−LiA	143.2(2)
N(2)−Fe−LiA	148.15(10)	N(3)−C(10)−N(2)	136.6(2)
N(4)−Fe−LiA	52.23(10)	N(3)−C(10)−N(1)	114.79(18)
N(1)A−Fe−LiA	54.38(9)	N(2)−C(10)−N(1)	108.64(17)
N(1)−Fe−LiA	140.15(10)	N(6)−C(20)−N(5)	122.1(2)
C(10)−N(1)−C(1)	110.15(16)	N(6)−C(20)−N(4)	116.31(19)
C(10)−N(1)−FeA	117.62(12)	N(5)−C(20)−N(4)	121.48(19)
C(1)−N(1)−FeA	123.67(14)	N(6)−C(20)−LiA	54.58(15)
C(10)−N(1)−Fe	87.34(11)	N(5)−C(20)−LiA	160.59(19)
C(1)−N(1)−Fe	124.13(13)	N(4)−C(20)−LiA	64.57(15)
FeA−N(1)−Fe	87.09(6)	N(3)−Li−N(6)A	168.7(2)
C(10)−N(1)−Li	78.48(15)	N(3)−Li−N(4)A	125.3(2)
C(1)−N(1)−Li	84.38(15)	N(6)A−Li−N(4)A	65.94(14)
FeA−N(1)−Li	77.86(11)	N(3)−Li−N(1)	66.11(13)
Fe−N(1)−Li	151.29(13)	N(6)A−Li−N(1)	115.8(2)
C(10)−N(2)−C(4)	124.53(18)	N(4)A−Li−N(1)	94.38(15)
C(10)−N(2)−Fe	99.46(13)	N(3)−Li−FeA	101.59(16)
C(4)−N(2)−Fe	135.69(14)	N(6)A−Li−FeA	86.45(15)
C(10)−N(3)−C(7)	124.71(19)	N(4)A−Li−FeA	47.11(9)
C(10)−N(3)−Li	95.91(18)	N(1)−Li−FeA	47.76(8)
C(7)−N(3)−Li	138.52(19)	C(20)A−Li−FeA	69.37(11)
C(20)−N(4)−C(11)	115.60(17)	C(10)−Li−FeA	71.25(11)
C(20)−N(4)−Fe	117.89(14)	C(1)−Li−FeA	72.27(11)
C(11)−N(4)−Fe	126.20(14)		
C(20)−N(4)−LiA	81.05(16)		

of 1.315(3) Å for C(10)−N(3) corresponds to a C═N double bond. Some delocalization of the π bond does occur between C(10)−N(2), which exhibits a bond distance of 1.341(3) Å.

The guanidinate monoanion displays three different C−N bond distances consistent with its coordination to both Li and Fe. The C−N(H)(^{i}Pr) bond distance (C(20)−N(5)) is 1.376 Å while the C−N^{i}Pr distances are 1.385 (C(20)−N(4)) and 1.309 Å (C(20)−N(6)). The longer of these arises from the dual coordination of this nitrogen to both the Li cation and Fe(II).

Deprotonation reactions employing complex **1** may also provide a route to guanidine dianion formation. As noted above, the reaction of complex **1** with 1 equiv of a variety of alkylating reagents led to the reduction of the Fe(III) center and formation of the dinuclear complex **2** (Scheme 1). Complex **2** reacts with 2 equiv of MeLi to produce complex **5** (Scheme 2). However, when **1** was allowed to react with additional $LiCH_2SiMe_3$ the products were dependent on stoichiometry as shown in Scheme 3.

Reaction of **1** with 2 equiv of $LiCH_2SiMe_3$ resulted in the formation of the Fe(II) complex **6**.[13] There are two obvious results from this reaction. First the Fe(III) center, as anticipated, has undergone reduction to Fe(II). Second, one guanidinate ligand on each of two different Fe centers has engaged in a subsequent reaction while one of them has remained intact. Perhaps it is not surprising that **6** could also be prepared by the addition of 1 equiv of $LiCH_2SiMe_3$ to **2** implying that **2** lies on the reaction pathway from **1** to **6**.

A likely pathway for the transformation of **1** to **6** begins with the reduction of **1** by the first equivalent of LiR to generate **2**. The second equivalent of lithium reagent apparently promotes the coupling of two bridging guanidinates to yield a bridging biguanidinate dianion. This may occur by deprotonation of one of the bridging guanidinate ligands by the second equivalent of lithium reagent to generate a nitrogen-centered anion. Subsequent attack of this nucleophilic center at the central carbon of the other bridging guanidinate with release of an amido anion would generate the new dianionic ligand, $\{[(^i\text{PrN})_2\text{C}]_2\text{N}^i\text{Pr}\}^{2-}$, observed for **6**. This proposal leaves a chelating bidentate guanidinate monoanion for completion of the coordination sphere for each of the Fe(II) centers in the dinuclear complex observed for **6**.

Bonding parameters within the biguanidinate ligand $[(^i\text{PrN}_2\text{C})_2\text{N}^i\text{Pr}]^{2-}$ are consistent with the resonance representation in Scheme 3.[13] In particular, the π bonds within the ligand appear to be localized in the N(4)−C(19)−N(5) framework (N(4)−C(19) 1.336(7) Å, N(5)−C(19) 1.311(7) Å), and the N(6)−C(19) distance of 1.453(6) Å is similar to the other single CN bond distances within the molecule. Furthermore, the C(19) is planar and N(4) and N(5) deviate only slightly from planarity (Σ of angles = 357°). The two Fe atoms in **6** are separated by a distance of 4.945 Å.

Reaction of **1** with 4 equiv of $LiCH_2SiMe_3$ generated compound **7** (Scheme 3). Results of a structural determination of this product are presented in Tables 1 and 5. The asymmetric unit for **7** has the formula Li_2(THF)[Fe{(^{i}PrN)$_2$CN^{i}Pr}(CH_2SiMe_3)$_2$]; application of a crystallographic inver-

Scheme 3

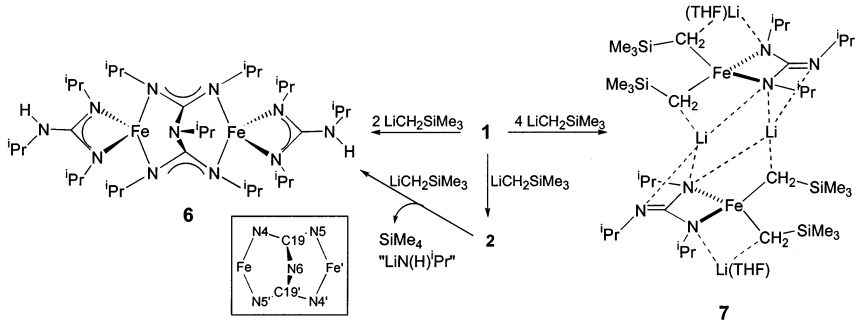

Table 5. Bond Lengths [A] and Angles [deg] for **7**

		Distances	
Fe−C(15)	2.095(4)	N(3)−C(7)	1.479(5)
Fe−C(11)	2.111(4)	C(1)−C(2)	1.519(5)
Fe−N(1)	2.119(3)	C(1)−C(3)	1.535(6)
Fe−N(2)	2.148(3)	C(4)−C(5)	1.517(5)
Li(1)−O(1)	1.860(9)	C(4)−C(6)	1.521(5)
Li(1)−N(2)	1.955(8)	C(7)−C(8)	1.500(6)
Li(1)−C(10)	2.758(9)	C(7)−C(9)	1.523(6)
Li(2)−N(3)	1.941(8)	C(11)−Si(1)	1.821(5)
Li(2)−N(1)A	2.059(8)	C(12)−Si(1)	1.842(6)
Li(2)−C(10)	2.608(8)	C(13)−Si(1)	1.875(7)
Li(2)−N(1)	2.714(8)	C(14)−Si(1)	1.854(5)
N(1)−C(10)	1.403(5)	C(15)−Si(2)	1.832(4)
N(1)−C(1)	1.476(5)	C(16)−Si(2)	1.805(11)
N(2)−C(10)	1.379(5)	C(17)−Si(2)	1.863(11)
N(2)−C(4)	1.474(5)	C(18)−Si(2)	1.842(11)
N(3)−C(10)	1.309(5)		
		Angles	
C(15)−Fe−C(11)	125.21(18)	Fe−N(1)−Li(2)	147.7(2)
C(15)−Fe−N(1)	104.46(14)	C(10)−N(2)−C(4)	122.2(3)
C(11)−Fe−N(1)	123.25(17)	C(10)−N(2)−Li(1)	110.4(4)
C(15)−Fe−N(2)	122.23(15)	C(4)−N(2)−Li(1)	115.3(4)
C(11)−Fe−N(2)	103.38(15)	C(10)−N(2)−Fe	93.6(2)
N(1)−Fe−N(2)	63.67(12)	C(4)−N(2)−Fe	128.4(2)
C(15)−Fe−Li(1)	163.7(2)	Li(1)−N(2)−Fe	78.0(3)
C(11)−Fe−Li(1)	57.5(2)	C(10)−N(3)−C(7)	121.6(3)
N(1)−Fe−Li(1)	82.8(2)	C(10)−N(3)−Li(2)	105.1(3)
N(2)−Fe−Li(1)	47.66(19)	C(7)−N(3)−Li(2)	132.5(3)
C(15)−Fe−Li(2)A	56.88(19)	N(1)−C(1)−C(2)	107.9(3)
C(11)−Fe−Li(2)A	152.6(2)	N(1)−C(1)−C(3)	111.9(3)
N(1)−Fe−Li(2)A	47.76(17)	C(2)−C(1)−C(3)	110.0(4)
N(2)−Fe−Li(2)A	94.13(17)	N(2)−C(4)−C(5)	107.7(3)
Li(1)−Fe−Li(2)A	129.7(2)	N(2)−C(4)−C(6)	111.3(3)
O(1)−Li(1)−N(2)	134.8(4)	C(5)−C(4)−C(6)	111.0(4)
O(1)−Li(1)−Fe	167.2(5)	N(3)−C(7)−C(8)	111.0(4)
N(2)−Li(1)−Fe	54.3(2)	N(3)−C(7)−C(9)	108.6(4)
O(1)−Li(1)−C(10)	123.9(4)	C(8)−C(7)−C(9)	109.9(4)
N(2)−Li(1)−C(10)	27.95(16)	N(3)−C(10)−N(2)	132.6(4)
Fe−Li(1)−C(10)	58.72(18)	N(3)−C(10)−N(1)	119.5(3)
N(3)−Li(2)−N(1)A	137.2(4)	N(2)−C(10)−N(1)	108.0(3)
N(3)−Li(2)−C(10)	28.98(16)	N(3)−C(10)−Li(2)	45.9(2)
N(1)A−Li(2)−C(10)	115.4(3)	N(2)−C(10)−Li(2)	157.6(3)
N(3)−Li(2)−N(1)	57.6(2)	N(1)−C(10)−Li(2)	78.9(3)
N(1)A−Li(2)−N(1)	99.1(3)	N(3)−C(10)−Li(1)	131.0(3)
C(10)−Li(2)−N(1)	30.48(13)	N(2)−C(10)−Li(1)	41.6(3)
N(3)−Li(2)−FeA	161.8(4)	N(1)−C(10)−Li(1)	91.8(3)
N(1)A−Li(2)−FeA	49.62(18)	Li(2)−C(10)−Li(1)	160.7(3)
C(10)−Li(2)−FeA	165.0(3)	Si(1)−C(11)−Fe	118.9(2)
N(1)−Li(2)−FeA	140.1(3)	Si(2)−C(15)−Fe	119.9(2)
N(3)−Li(2)−Li(2)A	91.0(4)	O(1)−C(19)−C(20)	106.5(6)
N(1)A−Li(2)−Li(2)A	58.7(2)	C(21)−C(20)−C(19)	105.5(6)
C(10)−Li(2)−Li(2)A	62.3(3)	C(20)−C(21)−C(22)	107.4(6)
N(1)−Li(2)−Li(2)A	40.41(19)	O(1)−C(22)−C(21)	107.1(5)
FeA−Li(2)−Li(2)A	103.8(3)	C(16)−Si(2)−C(18)	106.5(7)
C(22)−O(1)−C(19)	107.2(4)	C(18)−Si(2)−C(17)	108.2(8)
C(22)−O(1)−Li(1)	126.4(4)	C(16)−Si(2)−C(15)	111.6(4)
C(19)−O(1)−Li(1)	126.3(4)	C(15)−Si(2)−C(18)	113.1(4)
C(10)−N(1)−C(1)	116.3(3)	C(16)−Si(2)−C(17)	106.0(7)
C(10)−N(1)−Li(2)A	119.3(3)	C(15)−Si(2)−C(17)	111.1(4)
C(1)−N(1)−Li(2)A	110.3(3)	C(11)−Si(1)−C(12)	111.7(3)
C(10)−N(1)−Fe	94.1(2)	C(11)−Si(1)−C(14)	113.0(2)
C(1)−N(1)−Fe	130.7(3)	C(12)−Si(1)−C(14)	108.9(3)
Li(2)A−N(1)−Fe	82.6(2)	C(11)−Si(1)−C(13)	110.2(3)
C(10)−N(1)−Li(2)	70.6(3)	C(12)−Si(1)−C(13)	107.4(4)
C(1)−N(1)−Li(2)	81.2(3)	C(14)−Si(1)−C(13)	105.3(3)
Li(2)A−N(1)−Li(2)	80.9(3)		

sion center generates the molecular structure depicted in Figure 4. Complex **7** is a unique iron hydrocarbyl species supported by a dianionic guanidinate ligand.

The coordination geometry for the Fe(II) center in **7** is derived from a pseudotetrahedron defined by N(1), N(2), C(11), and C(15) with an average intervertex angle of 107°.

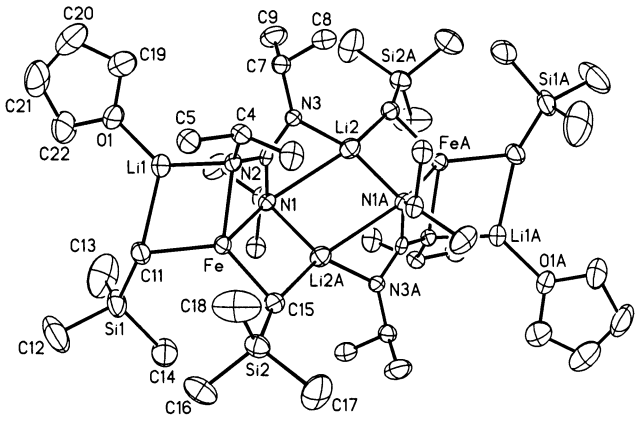

Figure 4. Molecular structure of $Li_4(THF)_2[Fe\{(^iPrN)_2CN^iPr\}(CH_2SiMe_3)_2]_2$ (**7**) with the atom numbering scheme. Hydrogen atoms have been omitted for clarity.

The largest distortion comes from the limited bite angle of the bidentate dianionic guanidinate ligand of 63.6(2)°. Within the guandinate ligand, the N(3)−C(10) bond distance of 1.310(6) Å indicates localization of π bonding between these two centers. The remaining two CN bond distances (N(2)−C(10) 1.381(6) Å, N(1)−C(10) 1.400(6) Å) are more consistent with a single bond between an sp^2 C and an sp^3 based N atom. This treatment essentially localizes the two negative charges of the dianion on N(1) and N(2) (Chart 1). Consistent with this assignment are the planar C(10) and N(3) centers and the coordination of the Fe(II) and the two Li countercations to N(1) and N(2).

The $[Fe\{(^iPrN)_2CN^iPr\}(CH_2SiMe_3)_2]^{2-}$ unit in complex **7** requires the presence of two Li countercations to attain neutrality. Figure 4 indicates their different environments. The Li(1)centers reside in a trigonal planar environment defined by the oxygen atom of an associated THF molecule, one of the negatively charged guanidinate nitrogen centers (N(2)), and a carbon of one of the CH_2SiMe_3 moieties (C(11)). The Li(2) cation assembles the two asymmetric units by bonding to two guanidinate nitrogen centers (N(1) and N(3)) within one anionic unit and a symmetry related nitrogen (N(1A)) and carbon center of a CH_2SiMe_3 moiety (C(15A)) in the associated asymmetric unit.

Although the mechanism for formation of **7** is apparently quite complicated it appears that 1 equiv of lithium reagent functions as a reducing agent to convert the Fe(III) center in **1** to the Fe(II) center observed in **7**. A second equivalent could be used to deprotonate a monoanionic guanidinate ligand and generate the dianionic ligand bonded to Fe in **7**. The final 2 equiv of $LiCH_2SiMe_3$ end up bonded to Fe. A loss of a lithium guanidinate or equivalent is necessary in this transformation.

Conclusion

We have demonstrated that Fe(II) and Fe(III) guanidinate complexes can be effectively prepared by reaction of lithium salts of *N*,*N*′,*N*″-tricyclohexylguanidinate and *N*,*N*′,*N*″-triisopropylguanidinate with the appropriate iron halide. Several attempts to prepare bis(guanidinato)iron(III) hydrocarbyl complexes led to isolation of Fe(II) species indicating the

preference of this oxidation state with the current ligand system. Structural examination of the Fe(II) guanidinate complexes **2**−**7** indicates a tendency for this ligand system to support four-coordinate distorted pseudotetrahedral geometries which in turn leads to dominance of dinuclear species generated through previously unobserved bridging interaction of the guanidinate ligand.

Metal-bound guanidinate ligands can be transformed into dianionic species or prompted to undergo coupling reactions to generate biguanidinate ligands by deprotonation with strong bases. This report continues to demonstrate the structural and electronic flexibility of the guanidinate ligand frame. We are currently exploring related chemistry with tetrasubstituted guanidinate and alkyl amidinate ligands.

Experimental Section

General Procedure. All reactions were carried out in a nitrogen-filled drybox. Diethyl ether, THF, hexane, toluene, and pentane were distilled under nitrogen from Na/K alloy. $FeBr_2$, $FeCl_3$, ^tBuLi (1.7 M in hexane), MeLi (1.4 M in hexane), $LiCH_2SiMe_3$, BzMgCl, Et_2Zn, diisopropylcarbodiimide, and dicyclohexylcarbodiimide were purchased from Aldrich and used without further purification. Infrared spectra were recorded with a Mattson Galaxy 3020 FTIR instrument as Nujol mulls. Magnetic susceptibilities were measured at room temperature in a Gouy balance (Johnson-Matthey) on samples prepared in sealed tubes in a drybox. Values were corrected for diamagnetism. Elemental analyses were run on a Perkin-Elmer PE CHN 4000 system.

FeCl{(^{i}PrN)$_2$C(HN^{i}Pr)}$_2$ (1). Triisopropylguanidine (1.212 g, 6.55 mmol) was dissolved in THF (50 mL). MeLi (4.68 mL, 1.4 M) was added to the solution dropwise. The solution was stirred for 15 min, followed by addition of 0.5 equiv of $FeCl_3$ (0.531 g, 3.27 mmol). The purple solution was stirred for 24 h at room temperature followed by removal of the solvent in vacuo. The product was extracted with pentane. Purple crystals were obtained from 15 mL of pentane at −30 °C (0.63 g, 42% yield). IR (Nujol): 3419(m), 3376(s), 1612(w), 1527(vs), 1484(vs), 1328(s), 1303(s), 1214(s), 1180(m), 1125(m), 994(m), 736(m), 689(m) cm^{-1}. Anal. Calcd for $C_{20}H_{44}N_6ClFe$: C, 52.23; H, 9.64; N, 18.27. Found: C, 52.03; H, 9.35; N, 18.06. μ_{eff} = 5.67 μ_B.

[Fe{μ-(^{i}PrN)$_2$C(HN^{i}Pr)}{(^{i}PrN)$_2$C(HN^{i}Pr)}]$_2$ (2). Triisopropylguanidine (0.500 g, 2.70 mmol) was dissolved in THF (40 mL). MeLi (1.93 mL, 1.4 M) was added to the solution dropwise. The solution was stirred for 15 min, followed by addition of 0.5 equiv of $FeBr_2$ (0.291 g, 1.35 mmol). The blue/green solution was stirred for 16 h at room temperature followed by removal of the solvent in vacuo. The product was extracted with pentane. Pale green crystals were obtained from 5 mL of pentane at −30 °C (0.47 g, 82% yield). IR (Nujol): 3426(m), 3397(w), 1650(m), 1532(vs), 1436(vs), 1311(s), 1176(m), 1133(m), 1075(w), 986(m), 838(w), 732(m) cm^{-1}. Anal. Calcd for $C_{20}H_{44}N_6Fe$: C, 56.59; H, 10.45; N, 19.80. Found: C, 56.95; H, 10.54; N, 20.10. μ_{eff} = 7.50 μ_B.

Reduction of FeCl{(^{i}PrN)$_2$C(HN^{i}Pr)}$_2$ (1) to [Fe{μ-(^{i}PrN)$_2$C(HN^{i}Pr)}{(^{i}PrN)$_2$C(HN^{i}Pr)}]$_2$ (2). To a solution of **4** in THF was added an alkylating reagent (1 equiv of BzMgCl, 0.5 equiv of Et_2Zn, 1 equiv of $LiCH_2SiMe_3$, or LiMe). The purple solutions were stirred overnight and filtered, and the solvent was removed in vacuo. Crystals of **5** were obtained from pentane as the sole isolable product in yields from 40 to 80%. Confirmation of **5** was done through comparison of unit cell parameters.

[Fe{μ-(CyN)$_2$C(HNCy)}{(CyN)$_2$C(HNCy)}]$_2$ (3). Tricyclohexylguanidine (1.00 g, 3.28 mmol) was dissolved in diethyl ether (30 mL). ^{n}BuLi (1.31 mL, 2.5M) was added to the solution dropwise. The solution was stirred for 15 min, followed by addition of 0.5 equiv of $FeBr_2$ (0.353 g, 1.64 mmol). The brown solution was stirred for 16 h at room temperature followed by removal of the solvent in vacuo. The product was extracted with pentane. Pale green crystals were obtained from 5 mL of pentane at −30 °C (0.80 g, 73% yield). IR (Nujol): 3458(m), 3420(w), 1652(m), 1534(vs), 1341(s), 1298(m), 1255(m), 1179(m), 1146(m), 1065(m), 1049(m), 978(w), 887(m) cm^{-1}. Anal. Calcd for $C_{38}H_{68}FeN_6$: C, 68.65; H, 10.31; N, 12.64. Found: C, 68.25; H, 10.01; N, 12.28. μ_{eff} = 7.28 μ_B.

[FeBr{μ-(CyN)$_2$C(HNCy)}]$_2$ (4). Tricyclohexylguanidine (0.500 g, 1.64 mmol) was dissolved in diethyl ether (30 mL). ^{n}BuLi (0.68 mL, 2.5 M) was added to the solution dropwise. The solution was stirred for 15 min, followed by addition of 1 equiv of $FeBr_2$ (0.353 g, 1.64 mmol). The brown/green solution was stirred for 16 h at room temperature. Pale crystals were obtained from 5 mL of diethyl ether at −30 °C (0.47 g, 82% yield). IR (Nujol): 3261(s), 3200(m), 1611(vs), 1248(m), 1151(m), 1099(m), 978(w), 890(m), 797(w), 713(w) cm^{-1}. Anal. Calcd for $C_{19}H_{34}BrFeN_3$: C, 51.84; H, 7.78; N, 9.54. Found: C, 52.16; H, 8.10; N, 9.32. μ_{eff} = 8.63 μ_B.

Li$_2$[Fe{μ-(^{i}PrN)$_2$C=N^{i}Pr}{(^{i}PrN)$_2$C(HN^{i}Pr)}]$_2$ (5). Dropwise addition of MeLi (0.97 mL, 1.4 M) to a solution of 0.570 g (0.671 mmol) of **5** dissolved in THF (20 mL) led to formation of a green solution. The reaction mixture was stirred for 16 h at room temperature and the solvent was removed in vacuo. The resultant solid was extracted with pentane. Pale yellow crystals were obtained from 3 mL of pentane at −30 °C (0.39 g, 68% yield). IR (Nujol): 3429(m), 1614(m), 1560(vs), 1538(vs), 1364(s), 1357(s), 1330(m), 1305(s), 1173(m), 1117(m), 1064(w), 1051(w), 988(m), 951(w), 932(w), 894(m), 850(m), 753(w) cm^{-1}. Anal. Calcd for $C_{20}H_{43}FeLiN_3$: C, 61.85; H, 11.16; N, 10.82. Found: C, 62.02; H, 10.88; N, 11.19. μ_{eff} = 7.51 μ_B.

Fe$_2${μ-(^{i}PrNCN^{i}Pr)$_2$(N^{i}Pr)}{(^{i}PrN)$_2$C(HN^{i}Pr)}$_2$ (6). Addition of 2 equiv of $LiCH_2SiMe_3$ (2.70 mL, 2.70 mmol, 1.0 M) to a solution of **1** (0.620 g, 1.35 mmol) in THF (50 mL) yielded a brown solution. The reaction mixture was stirred for 24 h at room temperature and filtered, and the solvent was removed in vacuo. Pale crystals were obtained from pentane at −30 °C (0.10 g, 19% yield). Anal. Calcd for $C_{35}H_{79}Fe_2N_{11}$: C, 54.90; H, 10.40; N, 20.12. Found: C, 55.00; H, 10.18; N, 19.93.

Li$_4$(THF)$_2$[Fe{(^{i}PrN)$_2$CN^{i}Pr}(CH$_2$SiMe$_3$)$_2$]$_2$ (7). Addition of 4.2 equiv of $LiCH_2SiMe_3$ (5.68 mL, 5.68 mmol, 1.0 M) to a solution of **1** (0.620 g, 1.35 mmol) dissolved in THF (50 mL) led to formation of a dark red solution. After being stirred for 48 h at room temperature, the reaction mixture was filtered and the solvent was removed in vacuo. Pale crystals were obtained from pentane at −30 °C (0.182 g, 27% yield). Anal. Calcd for $C_{22}H_{51}N_3OSi_2FeLi_2$: C, 52.89; H, 10.29; N, 8.41. Found: C, 52.58; H, 10.00; N, 8.08.

Structural Determination of 3·1.5(THF), 4, 5, and 7. Suitable crystals were selected, mounted on thin glass fibers with viscous oil, and cooled to the data collection temperature. Data were collected on a Bruker AX SMART 1k CCD diffractometer, using 0.3° ω-scans at 0, 90, and 180° in ϕ. Unit-cell parameters were determined from 60 data frames collected at different sections of the Ewald sphere. Semiempirical absorption corrections based on equivalent reflections were applied.[18]

No symmetry higher than triclinic was evident from the diffraction data of **3**·1.5(THF) and **5**. Solution in the centric option yielded chemically reasonable and computationally stable results of refine-

(18) Blessing, R. *Acta Crystallogr.* **1995,** A51, 33−38.

ment. Systematic absences in the diffraction data and unit-cell parameters were uniquely consistent for the reported space groups for **4** and **7**. The structures were solved by direct methods, completed with difference Fourier syntheses, and refined with full-matrix least-squares procedures based on F^2. The compound molecules for **4**, **5**, and **7** are located on inversion centers. Two tetrahydrofuran solvent molecules were located cocrystallized in the asymmetric unit of **3**·1.5(THF), one of which was at half-occupancy at an inversion center. Methyl groups of a trimethylsilyl moiety were found rotationally disordered with a site occupancy distribution of 60/40 in **7**. A cyclohexyl ring was found disordered with a roughly 50/50 site occupancy distribution in **3**·1.5(THF). All non-hydrogen atoms were refined with anisotropic displacement parameters. All hydrogen atoms were treated as idealized contributions. All scattering factors are contained in the SHEXTL 5.10 program library (Sheldrick, G. M., Bruker AXS, Madison, WI, 1997).

Acknowledgment. This work was supported by the Natural Sciences and Engineering Research Council of Canada.

Supporting Information Available: Tables of crystal data and structure solution and refinement details, atomic coordinates, bond lengths and angles, and anisoptropic thermal parameters for compounds **3**, **4**, **5**, and **7**. This material is available free of charge via the Internet at http://pubs.acs.org.

IC020088C